PHYSICS AND CHEMISTRY OF SOLID STATE
V. 25, No. 1 (2024) pp. 185-190
Section: Physics

DOI: 10.15330/pcss.25.1.185-190

Vasyl Stefanyk Precarpathian National University

ФІЗИКА І ХІМІЯ ТВЕРДОГО ТІЛА
Т. 25, № 1 (2024) С. 185-190
Фізико-математичні науки

PACS: 61.50.AH, 64.70FM

ISSN 1729-4428 (Print)
ISSN 2309-8589 (Online)

O.M. Matkivskyi[1], V.R. Balan[1], M.O. Halushchak[2], I.B. Dadiak[1], G.D. Mateik[2], I.V. Horichok[1]

Thermal conductivity of GeBiTe solid solutions

[1]*Vasyl Stefanyk Precarpathian National University, Ivano-Frankivsk, Ukraine, o.matkivsky@opora.org.ua*
[2]*Ivano-Frankivsk National Technical University of Oil and Gas Ivano-Frankivsk, Ukraine*

The paper calculates the electronic and lattice components of thermal conductivity coefficients for GeBiTe solid solutions. The calculation was carried out using two different models of the band structure of GeTe, which differ in the relative location of the zones of heavy and light holes. The first of the models is generally accepted for A^4B^6 compounds and assumes the location of the zone of light holes above the zone of heavy ones in the energy spectrum. Another model, obtained on the basis of DFT calculation, predicts the location of the zone of light holes below the zone of heavy ones. A significant difference was established in the numerical values of the electronic and lattice components of the thermal conductivity coefficients, depending on the adopted model. The influence of other calculation parameters on the investigated values was analyzed.

Keywords: germanium telluride, thermoelectric properties, coefficient of thermal conductivity.

Received 31 October 2023; Accepted 19 March 2024.

Introduction

Solid solutions based on germanium telluride are currently the best medium-temperature thermoelectric materials of p-type conductivity [1-10]. The highest values of thermoelectric factor were achieved for GePbBiTe solid solutions and consist about ≈ 2.3 at T = 700 K [2]. This value can be further improved, in particular by optimizing the doping process. However, the energy spectrum of carriers in solutions and its changes upon the introduction of impurities require a more detailed study.

The region of homogeneity of GeTe is one-sided and located on the chalcogen side. The maximum deviation from the stoichiometric composition is ≈ 1.5 at.% Te at a temperature of ≈ 700 K. The maximum melting temperature is – 998 K with an excess of Te ≈ 0.6 at.% [11]. The crystal lattice of germanium telluride is orthorhombic up to a temperature of about 680 K [1]. At higher temperatures - cubic, NaCl type. The unit cell parameter for the rhombohedral modification is 5.985 Å (α = 88.17º), and for the cubic 6.02 Å [10]. The phase transition temperature depends on the presence of impurities. In particular, [12] showed the possibility of stabilizing the cubic modification upon the introduction of 0.05 mol. % $AgInTe_2$.

As for other semiconductors of the A^4B^6 group, GeTe is characterized by a complex structure of the valence band. The set of experimental data is usually explained by taking into account two subzones, the distance between which depends on the temperature. However, the information on the numerical values of the characteristics of the band spectrum is incomplete. And the data of different authors do not always agree with each other [1, 2, 5, 10, 13-15].

In particular, according to [15], the valence band consists of a subband of light and heavy holes. At the same time, the extremum of the first of them at 300 K is 0.23 eV higher than that of the second. As the temperature increases, the distance between the subzones decreases with a temperature coefficient of $3 \cdot 10^{-4}$ eV/K. The effective mass of the density of states in the upper zone is ≈ 1.1 m_0, and according to the authors' conclusion, it does not depend on the carrier concentration. This arrangement of zones is generally accepted (characteristic) for many A^4B^6 compounds.

Instead, according to the calculation made in [1-2], in the rhombohedral phase, the zone of light holes is located

below the zone of heavy holes. At the same time, the width of the band gap and the distance between the extrema of the valence subbands differ from, for example, data [14]. In the cubic phase, according to [1-2], the zone of light holes is located above the zone of heavy ones, and the width of the band gap and the distances between the subbands are not so significantly different from [14]. It should be noted that according to calculations [1-2], the deformation of the cubic lattice leads to the fact that 6 out of 12 minima at point Σ of the Brillouin zone fall by ≈ 0.5 eV below the other six, and 1 out of 4 minima at point L of the Brillouin zone by ≈ 0.1 eV lower than the other three.

The effective mass of the density of states for the "upper" subzone determined by the authors [1] practically coincides with the value of 1.1 m_0 specified in [15]. The independence of the value of m^* from n, according to [15], may indicate that this zone is parabolic, and this will confirm the calculation [1-2].

In works [16, 17], when studying solid solutions GePbTe and GeBiTe, an approximation was used to calculate the electronic component of thermal conductivity, according to which the non-parabolic zone of light holes is located above. At the same time, the temperature dependence of the gap width was considered as presented in [14]. In these works [16, 17], important results were obtained regarding the location of the Fermi level. Based on them, the increase in ZT when Pb and Bi atoms were introduced into GeTe was explained. In view of the excellent numerical values of the zone parameters presented in [1-2] and used in [16, 17], in this work, based on experimental data [16-17], the calculation of the Fermi level and the electronic component of the thermal conductivity coefficient on their based on the purpose of establishing possible differences in the numerical values of these values due to the choice of the GeTe band structure model.

I. Calculation and analysis of results

The first stage in the calculation of the electronic component of thermal conductivity k_{el} is the determination of the chemical potential of electrons (Fermi level). By default, in [1-2, 16-17], these values are obtained from the experimental dependences of S(T). This calculation was carried out using the parabolic and non-parabolic valence band model, taking into account the possible degeneracy of carriers. For the non-parabolic zone in the two-band approximation [18]:

$$S = -\frac{k_0}{e_0}\left[\frac{I^1_{r+1,2}(\eta,\beta)}{I^0_{r+1,2}(\eta,\beta)} - \eta\right] \qquad (1)$$

where e_0 is the charge of the electron, $I^m_{n,k}(\eta,\beta)$ are the Fermi integrals, which according to [18], can be defined as follows:

$$I^m_{n,k}(\eta,\beta) = \int_0^\infty \left(-\frac{\partial f_0}{\partial x}\right)\frac{x^m(x+\beta x^2)^n dx}{(1+2\beta x)^k}.$$

In the presented expression $x = \frac{E}{k_0 T}$, $\eta = \frac{\mu}{k_0 T}$, $\beta = \frac{k_0 T}{E_g}$, $f_0 = \frac{1}{1+e^{x-\eta}}$, $-\frac{df_0}{dx} = \frac{e^{x-\eta}}{(1+e^{x-\eta})^2}$, μ is the chemical potential, r – current carrier dispersion parameter (r = 0 – correspond scattering on the deformation potential of acoustic (DA) and optical (DO) phonons, as well as the short-range potential of defects (SP); r = 1 – polarisation scattering on the optical phonons (PO); r = 2 – scattering on ionized defects (ID)) [18]. In the case of a parabolic zone, the β parameter in formula (1) should be set to zero.

The results of Fermi level calculations are presented in Fig. 1. It can be seen that the parabolic model predicts a deeper position of the Fermi level than the non-parabolic one. In the case of a non-parabolic zone, for two values of Eg(T) (from [2] and [14]), the value of μ differs by approximately 0.02 eV. At 500 K, it is about 40% ! In the range of temperatures corresponding to the existence of the cubic phase, the μ values differ less (since E_g according to [2] and [14] for this T range are close).

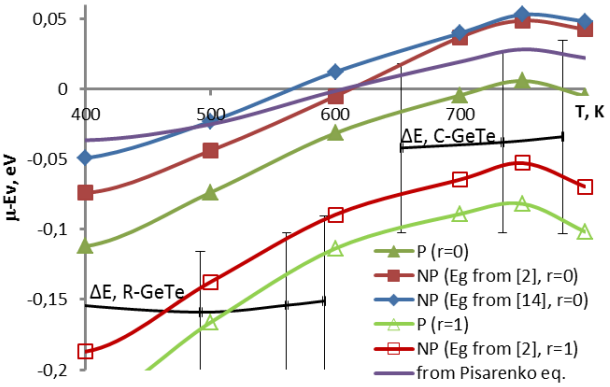

Fig. 1. The temperature dependence of the Fermi energy of $Ge_{0.96}Bi_{0.4}Te$ was determined from the experimental dependence of S(T) from [17] for various models (▲, Δ – parabolic valence band model; ■, □ – non-parabolic valence band model (E_g(T) – [2]); ♦ – non-parabolic valence band model (E_g(T) – [14]); curve without markers - parabolic band model and without taking into account carrier degeneracy (Pysarenko's formula)). "0" is taken as the position of the maximum of the upper valence subband. The relative position of the maximum of the lower valence band according to the work [1-2] is also given. The value of kT for different temperatures is shown in the form of an error scale.

For all calculation options for the R phase, the Fermi level is between the two zones. Therefore, it is worth considering both of them at the same time when analyzing properties. According to [2], in the case of simultaneous consideration of two zones, $S = \frac{S_1\sigma_1 + S_2\sigma_2}{\sigma_1+\sigma_2}$ That is, for this, the values of the effective masses and mobilities for each of the subzones are required.

It was established in [15] that at low concentrations of holes, their effective mass of the density of states is $m^* \approx 1m_0$, and at certain values of p it begins to increase due to the influence of the zone of heavy holes. Moreover, according to the authors' assumption, the most effective masses do not depend on the concentration.

It follows from the calculation [2] that for the rhombohedral phase of GeTe, the zone of heavy holes lies above the zone of light holes. (For most elements of groups A^4B^6, which crystallize in cubic lattices, the

opposite is true). Moreover, according to [2], the effective mass of the density of states in the zone of heavy holes is $m^* \approx 1.1m_0$, which is close to the data of [15]. It is worth noting that the authors of [2], when calculating the effective mass of the density of states, considered the anisotropy coefficient for the zone of heavy holes to be K= 6 without giving arguments. The number of minima at point Σ was considered equal to 6 (which corresponded to their calculations). Using the data obtained by the authors, calculated according to a similar scheme (that is, the number of minima at point L was considered equal to 3 and K= 6) the effective mass of the density of states of light holes is $m^* \approx 0.16m_0$.

Since the Fermi level is located between the extremes of the two valence bands, the concentration of holes will probably be mainly determined by the density of states of the upper band (that is, parabolic for the R-phase, and non-parabolic for the C-phase, if we accept the model [2]). However, it is known that kinetic effects are determined by electrons in the interval kT in the vicinity of the Fermi energy. And in the case of calculating the Fermi level for the R-phase, especially according to the parabolic zone model, μ turns out to be closer to the lower zone (non-parabolic L-zone with light holes).

Thus, without taking into account two zones at the same time, it will be difficult to obtain correct values of μ for the R-phase. Since the data on the position of the maxima of the Σ and L zones (as well as the values of m^* in them) would be worth confirming additionally, we did not calculate the Fermi level taking into account the two zones at the same time. In addition, the mechanisms and corresponding parameters for calculating mobilities in each of the zones in particular are unknown. Thus, the error in determining the Fermi energy according to one or another model will give certain extreme possible values with a difference of several tens of percent.

For the C-phase, for the parabolic zone model, the Fermi level is close to zero (that is, it practically coincides with the maximum of the upper zone). And in the case of a non-parabolic one, it is located higher than it by ≈ 0.05 eV. At the same time, both the distances between the subzones and the distance between the zones and the calculated values of the Fermi level are smaller than the value of kT. That is, as for the R-phase, it is necessary to take into account both zones.

Thus, unlike other A^4B^6 compounds, for which it is possible to separate the influence of zones in different temperature intervals, for GeTe it is obviously necessary to take into account both zones in the entire temperature interval.

It was interesting from a methodological point of view to analyze the values of μ(T) obtained when using the Pysarenko formula obtained in the parabolic zone approximation without taking into account degeneracy to determine the Fermi level: $S = -\frac{k_0}{e_0}[r + 2 - \eta]$. As can be seen from Fig. 1, in this case, the values of μ are overestimated (compared to the other considered models) for the R-phase, and underestimated for the C-phase. That is, the function μ(T) is smoother in the studied temperature interval.

The analysis of one more parameter of the calculation theory - the carrier scattering mechanism - deserves special attention. In most works, when interpreting the properties of GeTe and solid solutions based on it, it is assumed that holes are scattered by acoustic phonons. In this case, the parameter r is considered equal to zero. For most A^4B^6 compounds, this approach is justified. However, in [1] it is shown that for GePbBiTe solid solutions only up to ≈ 400 K the dependence $\mu(T) \sim T^{-3/2}$ is characteristic of the mechanism of carrier scattering by acoustic phonons. For impurity-free GeTe, this interval can be conditionally accepted up to 500 K. However, at higher T, the experimental data differ significantly from this approximation.

If we plot the logarithmic dependence of conductivity on temperature for the data σ(T) from [17], then up to the temperature corresponding to the phase transition we will get a straight line with a slope close to -3/2 (-1.35) (Fig. 2,a). That is, if *n* does not change with temperature, then it can be assumed that acoustic phonons are the dominant mechanism of carrier scattering. However, it was shown in [16] that for GePbTe the p_H slightly decreases with increasing temperature (it is worth noting that when analyzing Hall data, it is necessary to consider that the Hall factor for GeTe can be significantly different

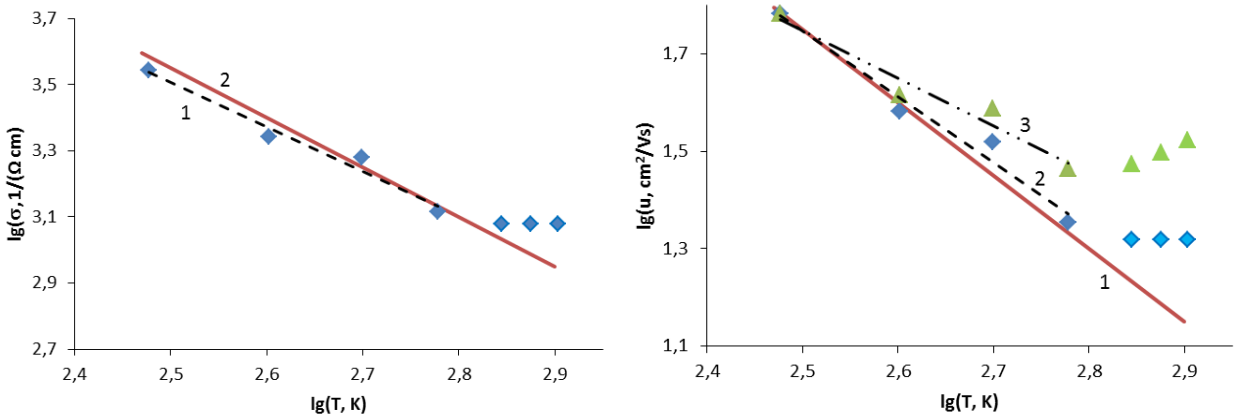

a) b)

Fig. 2. Temperature dependence of the specific electrical conductivity (a) and mobility (u = σ / e_0 p) (b) of the $Ge_{0.96}Bi_{0.4}Te$ sample (Experiment – [17]. In Fig. b: ♦ – the dependence of p(T) is not taken into account, ▲ – dependence p(T) is taken into account, according to [16]):
1 – theoretical line ~ (-3/2)·lg(T), 2 – approximation line ~ -1.35 lg(T), 3 – approximation line ~ -0.98 lg(T).

from unity [2]). Then, if we take into account that the concentration of carriers in the samples GeBiTe decreases slightly with increasing temperature with the same temperature coefficient of -2.73 10^{17} $cm^{-3}K^{-1}$ [16], then the dependence $\mu(T) \sim T^{-1}$ was calculated (Fig. 2, b).

The obtained result indicates either some influence of an additional scattering mechanism (in particular, at PO (r = 1) the slope should be -1/2), or the mass of carriers in the dominant zone depends on the position of the Fermi level. That is, the zone is non-parabolic and it is necessary to take into account the temperature dependence $m^*(\mu(T))$. In the case of non-parabolicity of the zone, with DA dominance, the slope should be -2.25, and with PO - -0.75 (according to [18]). All the discussed dependencies do not correspond to such values, and therefore, regardless of the type of zones, it is worth taking into account the possibility of simultaneously implementing several scattering mechanisms. At the same time, in addition to the mechanism of scattering on the polarization potential of optical phonons, which has a significant effect, in particular, in PbTe, for solid solutions based on GeTe, the contribution of scattering on a short-range potential or an ionized impurity can be significant. This is caused by a significant (up to 10 at.%) content of ionized impurity defects. In addition, the dielectric constant of GeTe [ε_∞ = 36 [19], ε_0 = 30.4 [20]] is not as large as, for example, PbTe [ε_∞ = 33 [21], ε_0 = 400 [21]]. Therefore, the shielding of the Coulomb field of ions will be much smaller.

If we still calculate the Fermi energy under the condition r = 1, then the calculated values of μ(T) will be located much deeper: 0.2 eV from the ceiling of the upper valence band at 300K (dashed curves in Fig. 1), compared to 0.1 eV at r = 0.

Despite the location of μ in the valence band (for all models), the value of the Lorentz constant is not very close to the value characteristic of a degenerate semiconductor (Fig. 3). L_0 was calculated according to the expression [18]

$$L_0(\eta,\beta) = \left(\frac{k_0}{e_0}\right)^2 \left[\frac{I^2_{r+1,2}(\eta,\beta)}{I^0_{r+1,2}(\eta,\beta)} - \frac{I^1_{r+1,2}(\eta,\beta)}{I^2_{r+1,2}(\eta,\beta)}\right]$$

In fact, when $\mu \approx E_v$ - 0.1 eV at T = 300 K, the product μ/kT ≈ 4. That is, according to [18], this is only a weak degeneracy. For various considered models, the maximum difference in the calculated values of L_0 is ≈ 30%. A similar difference is observed for kel calculated on its basis (Fig. 4). Thus, the choice of the model significantly affects the result of the kel calculation. k_{el} was calculated according to the Wiedemann-Franz law: $k_{el} = L_0 \sigma T$. At the same time, using experimental values of specific electrical conductivity. Non-monotonicities (local maxima) observed on some theoretical dependences kel(T) (Fig. 4) are most likely caused by the accumulation of error when taking into account the experimental dependences S(T) and σ(T) and should not appear in reality.

Such a possible discrepancy in the values of kel when using different model assumptions fundamentally affects the interpretation of klat (as the main parameter that researchers usually try to reduce in order to improve ZT), since the lattice component is usually defined as $k_{lat} = k_{tot} - k_{el}$. The k_{lat} values calculated in this way are shown in Fig. 5. The difference, for example, for the model of parabolic and non-parabolic zones at 400 K is ≈ 0.3 W/m K, i.e. ≈ 20%.

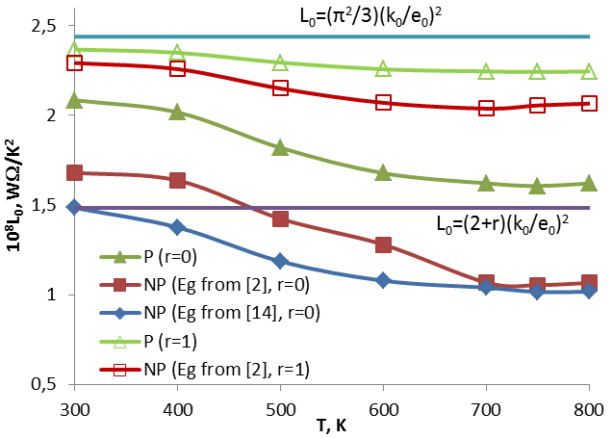

Fig. 3. The temperature dependence of the Lorentz number L_0 for $Ge_{0.96}Bi_{0.4}Te$ is calculated for various models based on the Fermi energy values shown in Fig. 1. The notations are the same:
(▲,Δ - parabolic valence band model; ■, □ – non-parabolic valence band model (E_g(T) – [2]); ♦ – non-parabolic valence band model (E_g(T) – [14])).

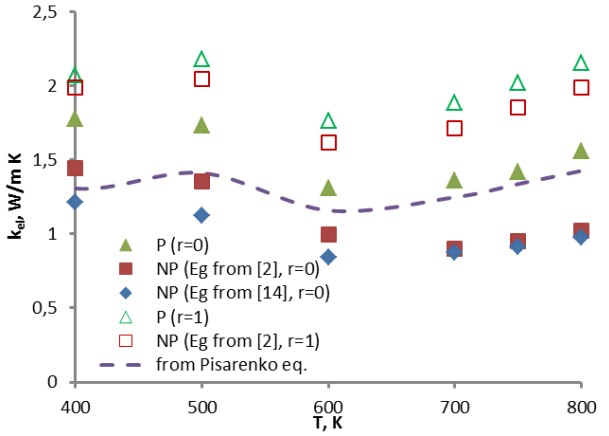

Fig. 4. The temperature dependence of the electronic component of the $Ge_{0.96}Bi_{0.4}Te$ thermal conductivity coefficient for different models is calculated based on the Fermi energy values shown in Fig. 1. Numerical values of σ(T) are taken from [17].
The symbols are the same (▲,Δ - parabolic valence band model; ■, □ – non-parabolic valence band model (E_g(T) – [2]); ♦ – non-parabolic valence band model (E_g(T) – [14]); curve without markers – a model of the parabolic zone and without taking into account carrier degeneracy (Pysarenko's formula).

Fig. 5 also shows two theoretical k_{lat}(T) curves. Each of them is obtained according to a typical calculation algorithm [or 1,2, 22], but with a different set of model parameters (θ, γ, ν). At the same time, both take into account the scattering of phonons on phonons and phonons on point defects. It can be seen that the curves are placed closer to the "experimental" values calculated on the basis of the non-parabolic model. And from the values obtained on the basis of the parabolic - much further. Thus,

in the second case, additional phonon scattering mechanisms should be taken into account to reconcile the calculation with the "experimental" values (ie, calculated as $k_{lat} = k_{tot} - k_{el}$).

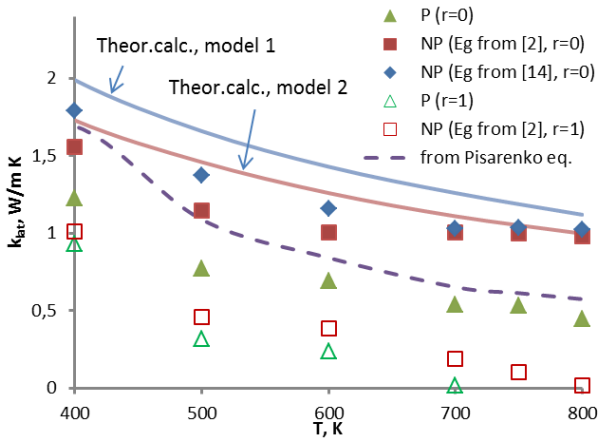

Fig. 5. Temperature dependence of the lattice component of the thermal conductivity coefficient of $Ge_{0.96}Bi_{0.4}Te$ for different models. The notations are the same: (▲,Δ – parabolic valence band model; ■, □ – non-parabolic valence band model ($E_g(T)$ – [2]); ♦ – non-parabolic valence band model ($E_g(T)$ – [14]); the curve without markers is a model of the parabolic zone without taking into account the degeneracy of the carriers (by Pisarenko). The figure also shows the curves corresponding to the theoretical calculation of k_{lat} (model 1 – parameters θ, γ, ν were selected from separate experiments, 2 – parameters θ, γ , ν were calculated on the basis of data on V_L, V_T [22]).

Thus, the calculation of kel will significantly influence the choice of model for the calculation of k_{lat}. This, in particular, can be seen in works [1, 2]. Thus, in particular, in [1] two mechanisms of phonon scattering are taken into account (scattering of phonons on phonons and phonons on point defects), and in [2] three additional mechanisms are taken into account (at grain boundaries, nanoinclusions, and scattering at packing defects). (Additionally, the authors of [1] and [2] also took into account N-processes. However, the ratio between U and N was used as a variation parameter).

Conclusions

1. GeTe-based solid solutions are weakly degenerate semiconductors and the calculation of their electronic properties, in particular the Fermi energy and the electronic component of the thermal conductivity coefficient, is sensitive to the choice of the band model and the numerical values of the band gap for the case of the non-parabolic band model. The difference between the estimated values of kel can be ≈ 30% with different calculation models.

2. Some parameters of the zone structure of GeTe and solid solutions require additional experimental studies, in particular, experimental confirmation of the mutual location of light and heavy hole zones, establishment of the dominant scattering mechanism of light and heavy holes and their effective masses.

Matkivskyi O.M. – Candidate of Physical and Mathematical sciences, senior researcher;
Balan V.R. – PhD student;
Halushchak M.O. – Doctor of Physical and Mathematical Sciences, Professor;
Dadiak I.B. – MS of Physics and Astronomy;
Mateik G.D. – Candidate of Physical and Mathematical Sciences, Associate Professor;
Horichok I.V. – Doctor of Physical and Mathematical Sciences, Professor.

[1] J. Li, X. Zhang, Z. Chen, S. Lin, W. Li, J. Shen, I.T. Witting, A. Faghaninia, Y. Chen, A. Jain, L. Chen, G.J. Snyder, Y. Pei, *Low-Symmetry Rhombohedral GeTe Thermoelectrics*, Joule, 2, 976 (2018); https://doi.org/10.1016/j.joule.2018.02.016.

[2] Min Hong, Zhi-Gang Chen, Lei Yang, Yi-Chao Zou, Matthew S. Dargusch, Hao Wang, and Jin Zou, *Realizing ZT of 2.3 in $Ge_{1-x-y}SbxInyTe$ via Reducing the Phase-Transition Temperature and Introducing Resonant Energy Doping*, Adv. Mater., 1705942 (2018); https://doi.org/10.1002/adma.201705942.

[3] S. Perumal, M. Samanta, T. Ghosh, U.S. Shenoy, A.K. Bohra, S. Bhattacharya et al, *Realization of High Thermoelectric Figure of Merit in GeTe by Complementary Co-doping of Bi and In*, Joule, 3, 2565(2019); https://doi.org/10.1016/j.joule.2019.08.017.

[4] S. Perumal, P. Bellare, U.S. Shenoy, U.V. Waghmare, and K. Biswas, *Low Thermal Conductivity and High Thermoelectric Performance in Sb and Bi Codoped GeTe: Complementary Effect of Band Convergence and Nanostructuring*, Chem. Mater., 29, 10426 (2017); https://doi.org/10.1021/acs.chemmater.7b04023.

[5] David J. Singh, *Optical properties of cubic and rhombohedral GeTe*, J. Appl. Phys., 113, 203101 (2013); https://doi.org/10.1063/1.4807638.

[6] Juan Li, Xinyue Zhang, Siqi Lin, Zhiwei Chen, and Yanzhong Pei, *Realizing the High Thermoelectric Performance of GeTe by Sb-Doping and Se-Alloying*, Chem. Mater., 29, 605 (2017); https://doi.org/10.1021/acs.chemmater.6b04066.

[7] A. Kumar, P. Bhumla, T. Parashchuk, S. Baran, S. Bhattacharya, and K.T. Wojciechowski, *Engineering Electronic Structure and Lattice Dynamics to Achieve Enhanced Thermoelectric Performance of Mn–Sb Co-Doped GeTe*, Chem. Mater. 33, 3611 (2021); https://doi.org/10.1021/acs.chemmater.1c00331.

[8] Y. Gelbstein, Z. Dashevsky, M.P. Dariel, *Highly efficient bismuth telluride doped p-type $Pb_{0.13}Ge_{0.87}Te$ for thermoelectric applications*, Phys. Status Solidi RRL – Rapid Research Letters, 1, 232 (2007); https://doi.org/10.1002/pssr.200701160.

[9] Y. Gelbstein, J. Davidow, *Highly efficient functional $Ge_xPb_{1-x}Te$ based thermoelectric alloys*, Phys. Chem. Chem. Phys., 16, 20120 (2014); https://doi.org/10.1039/C4CP02399D.
[10] Y. Gelbstein, J. Davidow, E. Leshem, O. Pinshow, and S. Moisa, *Significant lattice thermal conductivity reduction following phase separation of the highly efficient $Ge_xPb_{1-x}Te$ thermoelectric alloys*, Phys. Status Solidi B, 251(7), 1431 (2014); https://doi.org/10.1002/pssb.201451088.
[11] L.E. Shelimova, N.H. Abrikosov, V. V. Zhdanov, *Ge-Te system in the GeTe compound*, Journ. Inojg. Chem., 10(5), 1200 (1965).
[12] Z. Liu, N. Sato, Q. Guo, W. Gao, T. Mori, *Shaping the role of germanium vacancies in germanium telluride: metastable cubic structure stabilization, band structure modification, and stable N-type conduction*, NPG Asia Mater., 12, 1 (2020); https://doi.org/10.1038/s41427-020-00247-y.
[13] A. Edwards, *Theory of Intrinsic Defects in Crystalline GeTe and of Their Role in Free Carrier Transport*. Final Report, Kirtland: Air force research laboratory (2008).
[14] P.I. Konsyn, *Temperature dependences of the band gap and electronic spectra of ferroelectric semiconductors of the A^4B^6 type*, Solid State Physics, 24(5), 1321 (1982).
[15] L.M. Sysoeva, E.Ya. Lev, N.V. Kolomoets, *Changing the energy spectrum of germanium telluride current carriers by creating solid solutions based on it*, Physics of Thin Films, 3(4), 604 (1969).
[16] T. Parashchuk, A. Shabaldin, O. Cherniushok, P. Konstantinov, I. Horichok, *Origins of the enhanced thermoelectric performance for p-type $Ge_{1-x}Pb_xTe$ alloys*, Physica B: Condensed Matter, 596(46), 412397 (2020); https://doi.org/10.1016/j.physb.2020.412397.
[17] Z. Dashevsky, I. Horichok, M. Maksymuk, A. R. Muchtar, B. Srinivasan, T. Mori, *Feasibility of high performance in p-type $Ge_{1-x}Bi_xTe$ materials for thermoelectric modules*, J. Am. Ceram. Soc., 1 (2022); https://doi.org/10.1111/jace.18371.
[18] B.M. Askerov, Electron Transport Phenomena in Semiconductors, (1994); https://doi.org/10.1142/1926.
[19] P.B. Littlewood, *Phase transitions and optical properties of IV-Vl compounds*, Cond-Mat. Mtrl.-Sci, 48, 238 (2007).
[20] P.M. Nicolic, *Some optical propperties of lead-tin-chalcogenide alloys*, Matematica i fizika, 354 (1971).
[21] Y.I. Ravich, B.A. Efimova, I.A. Smirnov, *Semiconducting Lead Chalcogenides.* Ed. By L. S. Stil'bans, Springer Science+Business Media New York (1970). https://doi.org/10.1007/978-1-4684-8607-0.
[22] O.Z Khshanovska, M.O. Halushchak, O.M. Matkivskyi, I.V. Horichok, *Analysis of heat conductivity mechanisms in PbSnTe solid solutions*, Physics and Chemistry of Solid State, 24(3), 564 (2023); https://doi.org/10.15330/pcss.24.3.564-577.

О.М. Матківський[1], В.Р. Балан[1], М.О. Галущак[2], І.Б. Дадяк[1], Г.Д. Матеїк[2], І.В. Горічок[1]

Теплопровідність твердих розчинів GeBiTe

[1]Прикарпатський національний університет імені Василя Стефаника, Івано-Франківськ, Україна, o.matkivsky@opora.org.ua
[2]Івано-Франківський національний технічний університет нафти і газу, Івано-Франківськ, Україна

В роботі проведено розрахунок електронної та граткової складової коефіцієнтів теплопровідності для твердих розчинів GeBiTe. Розрахунок проведено з використанням двох відмінних моделей зонної структури GeTe, які відрізняються взаємним розташуванням зон важких та легких дірок. Перша з моделей є загальноприйнятою для сполук A^4B^6 та передбачає розташування зони легких дірок над зоною важких у енергетичному спектрі. Інша модель, отримана на основі DFT розрахунку, передбачає розташування зони легких дірок нижче зони важких. Встановлена значна відмінність в числових значення електронної та граткової складової коефіцієнтів теплопровідні в залежності від прийнятої моделі. Проаналізовано вплив інших параметрів розрахунку на досліджувані величини.

Ключові слова: телурид германію, термоелектричні властивості, коефіцієнт теплопровідності.